Rotor Blade Aeroelasticity in Forward Flight with an Implicit Aerodynamic Formulation

R. Celi* and P. P. Friedmann†
University of California, Los Angeles, Los Angeles, California

This paper describes a new methodology for formulating the aeroelastic stability and response problem for helicopter rotor blades. The mathematical expressions for the aerodynamic loads need not be explicit functions of the blade displacement quantities. The methodology is combined with a finite-element model of the blade and a quasilinearization solution technique. The resulting computer program is used to study the behavior of blades with noncoincident elastic axis, aerodynamic centers, and centers of mass.

Nomenclature

A = vector of aerodynamic loads, Eq. (1)
$B^k(\psi)$ = homogeneous system matrix in Eq. (6) at the kth iteration of quasilinearization
c = blade chord
$f^k(\psi)$ = nonhomogeneous system vector in Eq. (6) at the kth iteration of quasilinearization
F_{NL} = right-hand side of the nonlinear equations of motion of the blade written in first-order form, Eq. (1)
h = increment for finite-difference calculation of aerodynamic derivatives, Eqs. (20–22)
L = matrix containing the linear structural and inertia terms in the blade equations of motion, Eq. (1)
m = number of normal modes used in the modal coordinate transformation and size of the vector $y(\psi)$
N = vector containing the nonlinear structural and inertia terms in the blade equations of motion, Eq. (1)
$q(\psi)$ = state vector in the blade equations of motion, Eq. (1)
x_A = offset between the aerodynamic center and the elastic axis, positive for aerodynamic center ahead of the elastic axis
x_I = offset between the center of mass and the elastic axis, positive for center of mass ahead of the elastic axis
$y(\psi)$ = vector of generalized coordinates of the blade
Z = vector containing the nonhomogeneous structural and inertia terms in the blade equations of motion, Eq. (1)
ζ_j = real part of characteristic exponent
λ_j = characteristic exponent
μ = advance ratio
ψ = blade azimuth angle
ω_j = imaginary part of characteristic exponent
ϕ = elastic torsional deformation of the blade, radians
$\Phi(2\pi)$ = transition matrix of the homogeneous, Eq. (9), at the end of one period
$(*)$ = derivative with respect to ψ
$(\ )^k$ = value at the kth iteration of quasilinearization

Received March 23, 1987; presented as Paper 87-0921 at the AIAA Dynamics Specialist Conference, Monterey, CA, April 9–10, 1987; revision received Feb. 12, 1988.

*Doctoral Candidate, Mechanical, Aerospace, and Nuclear Engineering Department; currently Assistant Professor, Department of Aerospace Engineering, University of Maryland, College Park, MD. Member AIAA.

†Professor and Chairman, Mechanical, Aerospace, and Nuclear Engineering Department. Associate Fellow AIAA.

Introduction

ROTARY wing aeroelasticity is a multidisciplinary field in which aerodynamics, structural dynamics, control theory, numerical analysis, and software engineering play important and interrelated roles. The past few years have seen particularly vigorous research efforts in each of these areas for the purpose of improving the quality of the analytical models used to predict the dynamic characteristics of advanced rotors.[1]

As increasingly sophisticated and accurate tools become available, the analyst needs to find an appropriate balance between model accuracy and implementation effort. A conflict often arises between the need for modeling the blade with the most accurate and sophisticated theoretical models available and the need for keeping the implementation effort reasonably low and the computational requirements within practical limits. Furthermore, the two phases of the treatment of the aeroelastic problem, formulation and solution, are often linked and limit the analyst's choices. An efficient and reliable solution technique may be compatible only with less sophisticated, or more cumbersome to derive, formulations; conversely, more accurate theoretical models may be used only if one is willing to pay the price of less effective algorithms and increased difficulty in result interpretation.

A thorough review of formulation and solution techniques for rotary-wing aeroelasticity problems is beyond the scope of the present study: comprehensive reviews have been published by Friedmann,[1,2] Johnson,[3] and Ormiston.[4]

In the past few years the finite-element method has emerged as a powerful method of formulating the equations of motion of the blade. Several different approaches appear in the literature. Friedmann and Straub[5-7] build the finite-element representation by applying Galerkin's method of weighted residuals to the equations of motion of the blade in partial differential form. Chopra and his co-workers[8-14] build the finite-element representation around Hamilton's principle, used as a variational principle. They analyze conventional blades and blades having multiple load paths at the root, composite, and circulation control blades. A different approach is used by Hodges and his co-workers in their computer program GRASP for the stability of coupled rotor-fuselage configurations in hover.[15,16] GRASP is based on a direct discretization of the principle of virtual work, which is augmented with a family of multibody constraints to rigorously treat realistic rotorcraft systems.

The power of the finite-element method lies in the flexibility it provides in the problem formulation phase: different kinds of structural, or aerodynamic, or inertia models can be easily incorporated in the same blade representation. To take full

advantage of the power of the finite-element method, however, close attention has to be paid to the integration of the formulation and solution phases of the problem.

One problem in the formulation of the equations of motion for a rotor blade is that the size of the equations rapidly grows with the sophistication of the model. Furthermore, explicit functional relationships between modeling quantities and blade displacement quantities must be available to be able to write the equations of motion. Such functional relationships are not always available, particularly for the aerodynamic loads where table lookup or implicit relations are used.

Two different approaches have recently been pursued to formulate aeroelastic problems. The first approach is the use of special computer programs to perform the algebraic manipulations required to formulate the equations of motion. References 17–19 describe the development and use of a special purpose code for the symbolic derivation of the blade equations of motion. The equations of motion are obtained using Hamilton's principle and are converted to ordinary differential equations using Galerkin's method. The nonlinear equations of motion are linearized about a time-dependent equilibrium position, and the stability of the linearized system is calculated using Floquet theory. These techniques effectively solve the problems created by the size of the equations of motion of the blade because they shift most of the burden of the formulation process from the analyst to the computer. However, the need for explicit functional relationships between the modeling quantities still remains.

An alternative approach to circumvent both the problem of the algebraic complexity of the equations of motion, and the need for explicit functional relationships in the model, was pursued by Done and his co-workers. They derive the equations of motion of the blade in matrix form using Lagrange's equations.[20,21] However, they do not write the energy expressions in full and do not carry out the algebraic manipulations needed to obtain all of the required derivative matrices. A computational scheme is set up instead, which assembles the energy expressions numerically, and computes the numerical values of the system mass, damping, and stiffness matrices, and load vector. A modal coordinate transformation is performed; the equations of motion are linearized about an equilibrium position. This equilibrium position is not obtained from the program, but it is provided as external input. Done's approach was used for both hover and forward-flight cases.

A similar approach is also followed by Hodges and his co-workers in the GRASP[15,16] computer program: the steady-state residuals and matrix coefficients of the aeroelastic beam finite-element equations again are generated numerically, and explicit algebraic expressions are not derived. GRASP is limited to dynamic problems in which equations with periodic coefficients do not appear.

This paper has the following objectives: 1) to present the methodology for a new, implicit formulation of the aeroelastic problem, characterized by considerable flexibility and versatility in the modeling of the blade aerodynamic loads, and 2) to present results for the stability and response, in forward flight, of rotor blades with noncoincident elastic axis, cross-sectional centers of mass, and aerodynamic centers that were obtained using this new methodology.

The integration of an implicit formulation of the aerodynamic model with a finite-element discretization technique, a quasilinearization solution technique, and advanced numerical analysis software makes the analysis described in this study a new powerful tool for the aeroelastic analysis of helicopter rotor blades. The implicit formulation, coupled with a finite-element discretization, provides great flexibility in the choice of the aerodynamic model and considerably reduces the implementation effort. Quasilinearization,[22] together with well-proven and efficient ordinary differential equation (ODE) solvers,[23–25] provides a robust and reliable numerical tool and keeps the computational requirements reasonable.

Problem Formulation and Solution Technique

This section describes briefly an aeroelastic stability and response analysis for an isolated rotor blade in steady, trimmed forward flight, in which an implicit formulation of the aerodynamic loads is used. This formulation is based on the consideration that a single-pass solution of the blade response, in hover or forward flight, is usually impossible because of the nonlinearity in the equations of motion. Therefore, iterative techniques must be used. At each iteration, these techniques produce an approximation to the blade response, which can be used to generate the numerical values of the modeling quantities for the next iteration. In this study, this formulation is used for the aerodynamic portion of the blade model only, although an extension to the structural and inertia operators is conceptually straightforward. Thus, the aerodynamic loads for a given iteration are constructed numerically from the approximate response of the previous iteration; the matrices of derivatives with respect to the generalized coordinates, required for the stability analysis, are computed using finite-difference approximations. The various functional expressions that make up the aerodynamic model are not combined and expanded algebraically; "explicit" algebraic expressions of the aerodynamic loads are no longer required; thus, the formulation presented in this study has been denoted "implicit."

The equations of motion of the blade are similar to those derived in Ref. 7 (in Ref. 7, however, only the subset corresponding to the flap-lag stability and response problem was implemented). The equations describe the coupled flap-lag-torsional motion of a flexible, homogeneous, isotropic blade, modeled as a Bernoulli-Euler beam undergoing small strains and moderate deflections. Thus, this aeroelastic problem contains geometrically nonlinear terms in the structural, inertia, and aerodynamic operators, which are due to nonlinear beam kinematics. The inertia loads are obtained using D'Alembert's principle. Quasisteady strip theory, with uniform inflow, is used in the aerodynamic model. Stall and compressibility effects are not included. The blade properties may have arbitrary, piecewise linear, spanwise distributions; in particular, the cross-sectional offsets of the center of mass and of the aerodynamic center, with respect to the shear center, need not be zero.

The spatial dependence of the equations of motion of the blade is eliminated by using a Galerkin method of weighted residuals.[5–7] This results is a finite-element discretization. Cubic interpolation polynomials are used for the modeling of flap and lag bending, quadratic interpolation polynomials for the modeling of torsion. The resulting finite-element has a total of 11 degrees of freedom: displacement and slope at each end of the element, for flap bending; displacement and slope at each end of the element, for lag bending; and rotation at each end of the element and a midelement node, for torsion. The axial degree of freedom is eliminated by assuming that the blade is inextensional. The partial differential equations of motion of the blade thus are transformed into a set of nonlinear, coupled, ordinary differential equations with periodic coefficients. A modal coordinate transformation is used to reduce the number of degrees of freedom of the system. A variable number of rotating coupled modes, usually six, are used in the modal coordinate transformation. The modes are calculated for a root pitch angle equal to the collective pitch.

The equations of motion of the blade are then rewritten in first-order form as follows:

$$\dot{q} = L(\psi)q + N(q, \overset{*}{q}; \psi) + Z(\psi) + A(q, \overset{*}{q}; \psi)$$
$$= F_{NL}(q, \overset{*}{q}; \psi) \tag{1}$$

The matrix $L(\psi)$ contains the linear portion of the blade model, the vector $N(q, \overset{*}{q}; \psi)$ the nonlinear terms, and the

vector $Z(\psi)$ the nonhomogeneous terms; $q(\psi)$ is the state vector defined as

$$q(\psi) = \begin{Bmatrix} y(\psi) \\ \overset{*}{y}(\psi) \end{Bmatrix} \tag{2}$$

The matrices $L(\psi)$, $N(q, \overset{*}{q}; \psi)$, and $Z(\psi)$ do not contain any aerodynamic contributions: these are all contained in the vector $A(q, \overset{*}{q}; \psi)$. The numerical value of $A(q, \overset{*}{q}; \psi)$ for given q, $\overset{*}{q}$, and ψ is known. However, its explicit algebraic form is not known. All of the matrices and vectors in Eq. (1) are periodic, with common period $T = 2\pi$. If m modes are used to perform the modal coordinate transformation, the system of ordinary differential equations, Eq. (1), has size $n = 2m$.

Let $q(\psi)^k$ be an approximate solution of Eq. (1). Quasilinearization[22] is based on performing a first-order Taylor series expansion of Eq. (1) about q^k:

$$\overset{*}{q}^{k+1} = \overset{*}{q}^{k} + \left(\frac{\partial F_{NL}}{\partial q}\right)^k (q^{k+1} - q^k) + \left(\frac{\partial F_{NL}}{\partial \overset{*}{q}}\right)^k (\overset{*}{q}^{k+1} - \overset{*}{q}^{k}) \tag{3}$$

in which

$$\left(\frac{\partial F_{NL}}{\partial q}\right)^k = L(\psi)q^k + \left(\frac{\partial N}{\partial q}\right)^k + \left(\frac{\partial A}{\partial q}\right)^k \tag{4}$$

$$\left(\frac{\partial F_{NL}}{\partial \overset{*}{q}}\right)^k = \left(\frac{\partial N}{\partial \overset{*}{q}}\right)^k + \left(\frac{\partial A}{\partial \overset{*}{q}}\right)^k \tag{5}$$

Equation (3) can be written in the form

$$\overset{*}{q}^{k+1} = B^k(\psi)q^{k+1} + f^k(\psi) \tag{6}$$

Comparing Eq. (3) and Eq. (6) one has

$$B^k(\psi) = \left[I - \left(\frac{\partial N}{\partial \overset{*}{q}}\right)^k - \left(\frac{\partial A}{\partial \overset{*}{q}}\right)^k\right]^{-1}\left[\left(\frac{\partial N}{\partial q}\right)^k + \left(\frac{\partial A}{\partial q}\right)^k + L(\psi)\right] \tag{7}$$

$$f^k(\psi) = \left[I - \left(\frac{\partial N}{\partial \overset{*}{q}}\right)^k - \left(\frac{\partial A}{\partial \overset{*}{q}}\right)^k\right]^{-1} \times \left\{Z + N^k + A^k - \left[\left(\frac{\partial N}{\partial q}\right)^k + \left(\frac{\partial A}{\partial q}\right)^k\right]q^k - \left[\left(\frac{\partial N}{\partial \overset{*}{q}}\right)^k + \left(\frac{\partial A}{\partial \overset{*}{q}}\right)^k\right]\overset{*}{q}^k\right\} \tag{8}$$

Equation (6) defines an iterative procedure; the sequence of Eq. (6) converges to the solution of the nonlinear system, Eq. (1).

The solution of Eq. (6) requires[22] the knowledge of the state transition matrix $\Phi^k(2\pi)$ of the homogeneous system

$$\overset{*}{q}^{k+1} = B^k(\psi)q^{k+1} \tag{9}$$

at the end of one period. The matrix $\Phi^k(2\pi)$ is computed using the following algorithm. Let $D^k(\psi)$ be a block-diagonal square matrix of size n^2 by n^2, defined as

$$D^k(\psi) = \begin{bmatrix} B^k(\psi) & & & 0 \\ & B^k(\psi) & & \\ & & \ddots & \\ 0 & & & B^k(\psi) \end{bmatrix} \tag{10}$$

Then solve the system

$$\overset{*}{z}(\psi) = D^k(\psi)z(\psi) \tag{11}$$

from $\psi = 0$ to $\psi = 2\pi$, with the initial condition vector $z(0)$ given by

$$z(0) = \begin{Bmatrix} e_1 \\ e_2 \\ \cdots \\ e_n \end{Bmatrix} \tag{12}$$

where e_i is a vector of size n with all of its elements equal to zero except for the ith, which is equal to 1. Let $z(2\pi)$ be the solution vector of Eq. (11) at $\psi = 2\pi$. Partition $z(2\pi)$ into n vectors of size n:

$$z(2\pi) = \begin{Bmatrix} z_1(2\pi) \\ z_2(2\pi) \\ \cdots \\ z_n(2\pi) \end{Bmatrix} \tag{13}$$

The ith column of the transition matrix $\Phi^k(2\pi)$ is then given by $z_i(2\pi)$, i.e.,

$$\Phi^k(2\pi) = [z_1(2\pi)\ z_2(2\pi) \ldots z_n(2\pi)] \tag{14}$$

This algorithm is the single-pass version of the classic n-pass algorithm[26] in which the columns of $\Phi^k(2\pi)$ are obtained by solving Eq. (9) n times, with initial condition vectors $q^{k+1}(0)$, $k = 1,2,\ldots,n$, which have all their elements equal to zero, except for the ith, which is equal to 1. The implementation of the algorithm does not require the actual coding of the n^2 by n^2 matrix $D^k(\psi)$. Only the coding of the n by n matrix $B^k(\psi)$ is needed. The initial condition vector $q^{k+1}(0)$ associated with Eq. (6) is not known a priori but can be identified by requiring that the solution be periodic with period 2π:

$$q^{k+1}(0) = q^{k+1}(2\pi) \tag{15}$$

The vector $q^{k+1}(0)$ is the solution of the linear algebraic system[27]

$$[I - \Phi^k(2\pi)]q^{k+1}(0) = \bar{q}^k(2\pi) \tag{16}$$

in which I is the identity matrix, and $\bar{q}^k(2\pi)$ is the solution vector of Eq. (6), integrated from $\psi = 0$ to $\psi = 2\pi$ with the initial condition vector $\bar{q}^k = 0$.

The stability of the system, linearized about the time-dependent equilibrium position $q^k(\psi)$ at the kth iteration, is determined from Floquet theory.[22] The characteristic exponents of the transition matrix $\Phi^k(2\pi)$

$$\lambda_j = \zeta_j \pm i\omega_j, \qquad j = 1,2,\ldots,m \tag{17}$$

are evaluated. The linearized system is stable if all the $\zeta_j < 0$.

In order to write Eqs. (3) and (6), one needs the derivatives of the aerodynamic vector $A(q, \overset{*}{q}; \psi)$ with respect to the state vector q (and $\overset{*}{q}$). Since the explicit algebraic form of A is not known, the derivatives are obtained as described below. The derivative matrices $[\partial A/\partial q]^k$ and $[\partial A/\partial \overset{*}{q}]^k$, both of size n by n, have the following form:

$$\left(\frac{\partial A}{\partial q}\right)^k = \begin{bmatrix} 0 & 0 \\ \left(\frac{\partial A}{\partial y}\right)^k & \left(\frac{\partial A}{\partial \overset{*}{y}}\right)^k \end{bmatrix} \tag{18}$$

$$\left(\frac{\partial A}{\partial \overset{*}{q}}\right)^k = \begin{bmatrix} 0 & 0 \\ 0 & \left(\frac{\partial A}{\partial \overset{**}{y}}\right)^k \end{bmatrix} \tag{19}$$

The derivative matrices $[\partial A/\partial y]^k$, $[\partial A/\partial \overset{*}{y}]^k$, and $[\partial A/\partial \overset{**}{y}]^k$ all have size m by m. They are functions of the blade azimuth

ψ and must be recalculated at each value of ψ required by the numerical integration routines, Since the explicit algebraic form of $A\ (q, \overset{*}{q}; \psi)$ as a function of y, $\overset{*}{y}$, and $\overset{**}{y}$ is not known, the derivatives are computed using a finite-difference approximation.

The ith column of the derivative matrix $[\partial A/\partial y]$ is the vector $\{\partial A/\partial y_i\}$ of derivatives of the aerodynamic load vector A with respect to the generalized coordinate y_i, with $i = 1,2,\ldots,n$. The vector $\{\partial A/\partial y_i\}$ at the kth iteration of quasilinearization, and at the azimuth $\psi = \psi_0$, is approximated by

$$\left\{\frac{\partial A}{\partial y_i}\right\}^k_{\psi=\psi_0} \approx \frac{1}{h}\left[A\left(y^k(\psi_0)+h, \overset{*}{y}{}^k(\psi_0), \overset{**}{y}{}^k(\psi_0);\psi_0\right) - A\left(y^k(\psi_0), \overset{*}{y}{}^k(\psi_0), \overset{**}{y}{}^k(\psi_0);\psi_0\right)\right]$$

$$i = 1,2,\ldots,m \tag{20}$$

where h is a vector with all its components equal to zero, except for the ith, which is equal to h. Similarly, the columns of $[\partial A/\partial \overset{*}{y}]$ and $[\partial A/\partial \overset{**}{y}]$ are given by

$$\left\{\frac{\partial A}{\partial \overset{*}{y}_i}\right\}^k_{\psi=\psi_0} \approx \frac{1}{h}\left[A\left(y^k(\psi_0), \overset{*}{y}{}^k(\psi_0)+h, \overset{**}{y}{}^k(\psi_0);\psi_0\right) - A\left(y^k(\psi_0), \overset{*}{y}{}^k(\psi_0), \overset{**}{y}{}^k(\psi_0);\psi_0\right)\right]$$

$$i = 1,2,\ldots,m \tag{21}$$

$$\left\{\frac{\partial A}{\partial \overset{**}{y}_i}\right\}^k_{\psi=\psi_0} \approx \frac{1}{h}\left[A\left(y^k(\psi_0), \overset{*}{y}{}^k(\psi_0), \overset{**}{y}{}^k(\psi_0)+h;\psi_0\right) - A\left(y^k(\psi_0), \overset{*}{y}{}^k(\psi_0), \overset{**}{y}{}^k(\psi_0);\psi_0\right)\right]$$

$$i = 1,2,\ldots,m \tag{22}$$

Results

Two basic configurations were considered for the forward-flight study: a soft in-plane and a stiff in-plane hingeless uniform blade configuration with uncoupled fundamental lag frequencies of 0.732/rev and 1.42/rev, respectively. For both baseline configurations, the uncoupled fundamental flap and torsion frequencies were 1.125/rev and 3.17/rev, respectively. The Lock number was $\gamma = 5.5$, the rotor solidity $\sigma = 0.07$, and the thrust coefficient $C_T = 0.005$. The blade precone angle β_p and the root offset e_1 were equal to zero. The modal coordinate transformation was based on the sixth lowest frequency, rotating, coupled modes of the blade. In all cases the six modes were one torsion, two lag, and three flap modes. The blades were modeled using five finite elements with nodes at 0%, 22.5%, 45%, 67.5%, 90% and 100% of the span. The trim procedure used in these calculations was a propulsive trim procedure identical to that used in Ref. 22. Unless otherwise specified, all of the results presented in this paper refer to these baseline configurations.

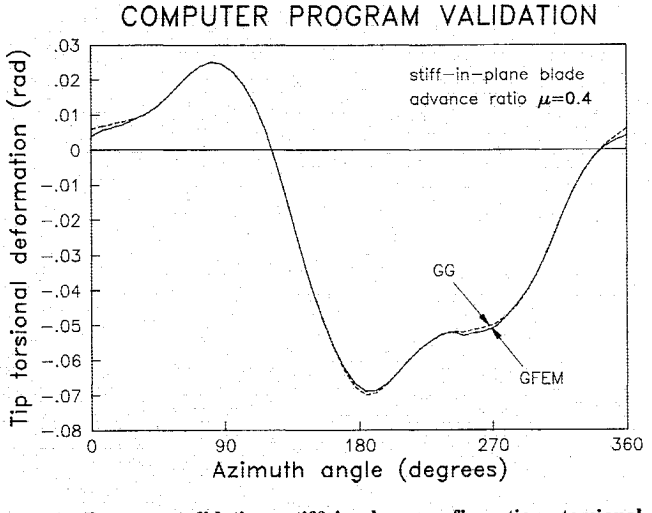

Fig. 1 Program validation; stiff in-plane configuration; torsional response of blade tip (GFEM: present method, GG: Ref. 22).

The finite-element aeroelastic analysis was validated by comparing its results with those of the analysis described in Ref. 22. Figure 1 is a representative plot obtained during these validation studies. In this plot the torsional response of the blade tip is presented as a function of the blade azimuth angle, for the stiff in-plane blade configuration, at an advance ratio $\mu = 0.4$. The shear center, the aerodynamic center, and the center of gravity are coincident. The curve marked with "GG" refers to the results obtained from the program developed in Ref. 21, which implements a classical, global Galerkin method. The curve marked with "GFEM" refers to the results of the Galerkin finite-element code described in this paper. During the validation, the modal coordinate transformation in the finite-element program was carried out using uncoupled blade modes, so as to maintain consistency with the global Galerkin analysis.

Table 1 shows a comparison between the real parts of the characteristic exponents computed using the present analysis and those computed using the analysis of Ref. 22. The blade configuration is the same as in Fig. 1.

Since the two computer programs implement exactly the same blade model in widely different fashions, the good agreement between these results provided confidence in the correctness of the implementation. It should be noted that results similar to Fig. 1 also were generated for the flap and lag degrees of freedom. However, since the agreement between the two sets of results was even better than those in Fig. 1, these results are not presented here and can be found in Ref. 27.

The finite-element program was used to analyze 12 different blade configurations. Some of the most interesting results of this study are presented in this paper. A considerable number of additional results can be found in Ref. 27. Aeroelastic stability and response were calculated, for each configuration, in hover and at four values of the advance ratio in forward flight, for a total of 48 complete quasilinearization procedures. Each procedure required between two and four iterations to converge, for an overall total of 160 iterations. The rate of convergence was not affected by the level of damping of the system. The initial approximation to the response, in all cases, was to set all of the displacement quantities to zero (i.e., a rigid blade initial approximation was used). Quasilinearization converged in all cases. Comparison runs with the program of Ref. 22 showed that the explicit and the implicit formulations lead to exactly the same iteration history: both the stability and the response results of each iteration coincide.

Table 1 Finite-element program validation, comparison of real parts of characteristic exponents, stiff in-plane uniform blade, zero cross-sectional offsets and precone, two uncoupled modes per degree of freedom, advance ratio $\mu = 0.4$

Mode type	(A) Present work	(B) Ref. 22	$\frac{(A)-(B)}{(B)}$ %
First lag	0.02334	0.02280	2.4
Second lag	−0.01376	−0.01550	11.2
First flap	−0.3819	−0.3807	0.3
Second flap	−0.2116	−0.2081	1.7
First torsion	−0.3943	−0.3959	0.4
Second torsion	−0.2226	−0.2207	0.9

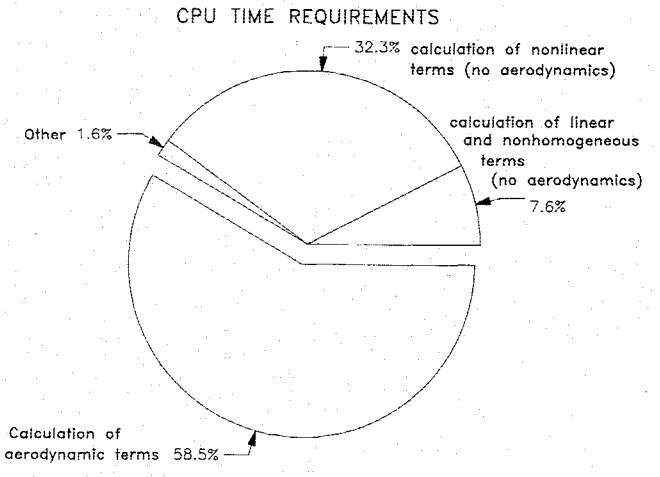

Fig. 2 CPU time requirements—percent of total CPU time spent on each phase; implicit formulation.

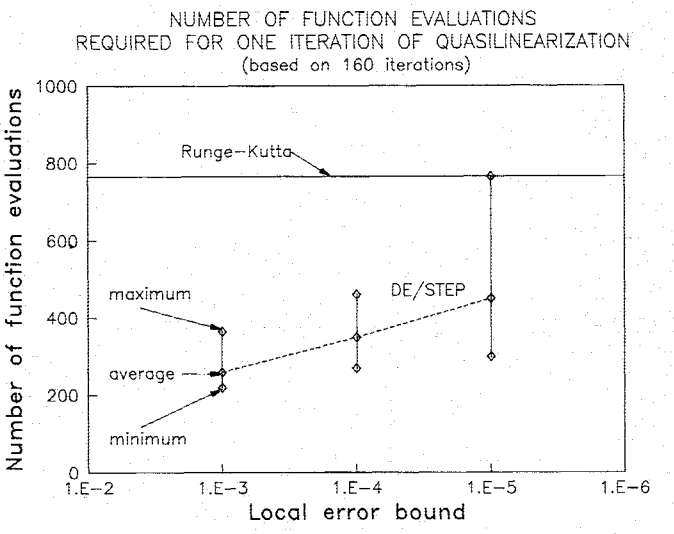

Fig. 3 Number of function evaluations required for one iteration of quasilinearization.

Figure 2 shows the distribution of CPU time on the average among the various phases of the solution process, calculation of the linear and nonhomogeneous structural and inertia terms, of the nonlinear structural and inertia terms, and the aerodynamic terms. The portion marked "Other" includes the calculation of the mode shapes and frequencies of the blade and the overhead associated with the solution of the ODE. "Overhead" refers to the operations required to advance the ODE by one time step, once all the system matrices have been calculated and assembled, and the modal coordinate transformation has been performed. This is the only portion of the program that benefits from the reduction in degrees of freedom brought about by the modal coordinate transformation. Furthermore, this portion required only a minuscule percentage of the overall CPU time. This also suggests that in future studies the solution of the complete finite-element equations, with all the nodal degrees of freedom retained, would be both feasible and practical.

An accurate comparison between the computational efficiency of the explicit and of the implicit formulation is not easy to make because a coupled flap-lag-torsion finite-element analysis using an explicit formulation was not implemented. The implicit formulation is somewhat less efficient than the explicit one because of the need to build finite-difference approximations to several derivative matrices that appear in the solution process. On the other hand, the calculation of the aerodynamic loads at a given blade azimuth angle and radial station is faster with an implicit formulation because the expressions for the loads are more compact. Based on extrapolations from the flap-lag finite-element code described in Ref. 15, an implicit formulation requires 10–15% more CPU time than an explicit formulation, all other aspects of the implementation being equal.

The code used to integrate the equations of motion was DE/STEP, a general purpose Adams-Bashforth ODE solver, which tends to be particularly convenient when the right-hand side of the system of equations is expensive to evaluate.[23-25] Fig. 3 shows the number of function evaluations required to perform one iteration of quasilinearization. The data are based on a collection of 160 iterations. At each integration step, DE/STEP computes an estimate e_L of the local error. The step is considered sufficiently accurate if $e_L \leq e_R q_i + e_A$, in which e_R and e_A are the user-specified relative and absolute error tolerances for each component q_i of the solution vector $q(\psi)$. For all of the results presented in this study $e_A = e_R$. In Fig. 3 the minimum, average, and maximum number of function evaluations required are plotted as a function of the local relative error bound used by DE/STEP. One function

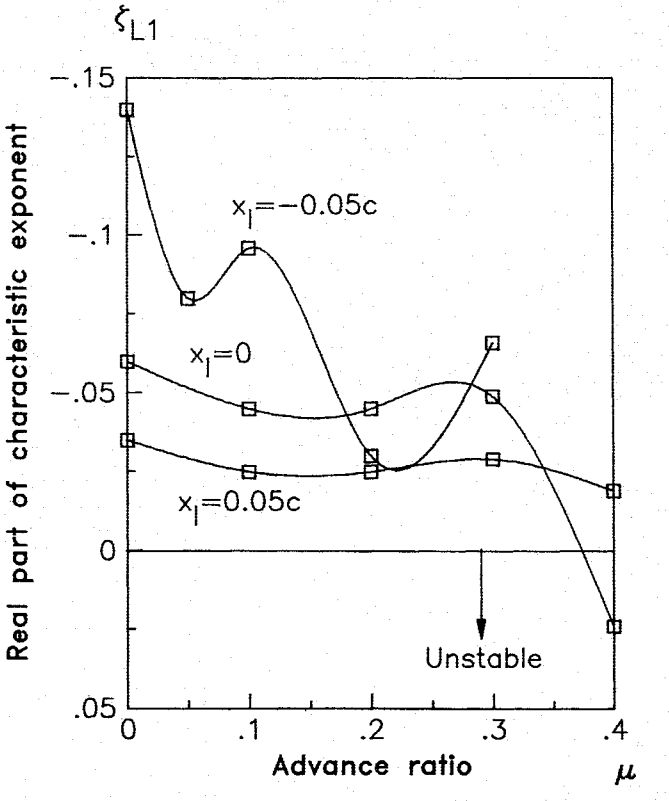

Fig. 4 Stiff in-plane configuration stability; first lag mode; real part of characteristic exponent vs μ.

evaluation consists of the calculation of the right-hand side of Eq. (6), or one evaluation of the right-hand side of Eq. (11). Also shown is the (fixed) number of function evaluations required in the implementation of Ref. 22. A value of $e_R = 10^{-3}$ produced acceptable accuracy in most cases. Figure 3 shows that, with a judicious choice of the ODE solver, relatively large gains in computational efficiency can be obtained with minimum implementation effort.

Figures 4 and 5 show results for three stiff in-plane blade configurations: one in which the elastic axis (EA) and the line of cross-sectional centers of mass (CG) are coincident, a second with a positive CG-EA offset x_I equal to 5% of the blade chord, and the third with the same amount of offset, but negative. The CG-EA offset x_I is positive if the CG is ahead of the EA.

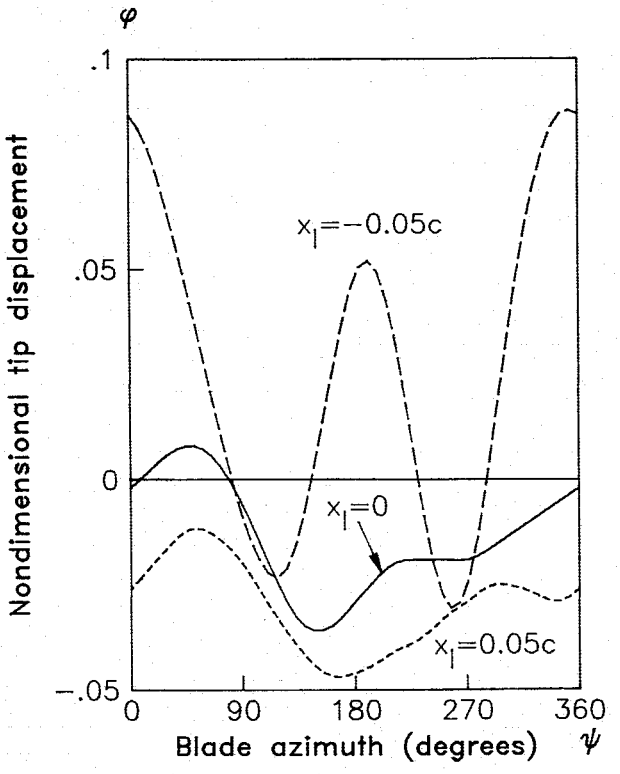

Fig. 5 Stiff in-plane blade configuration; torsional response of the blade tip; advance ratio $\mu = 0.3$.

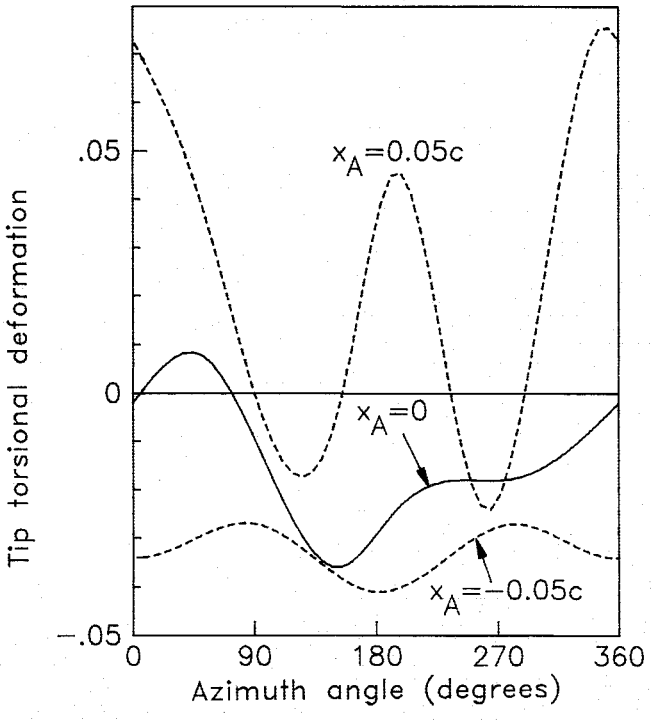

Fig. 7 Stiff in-plane blade configuration; torsional response of the blade tip; advance ratio $\mu = 0.3$.

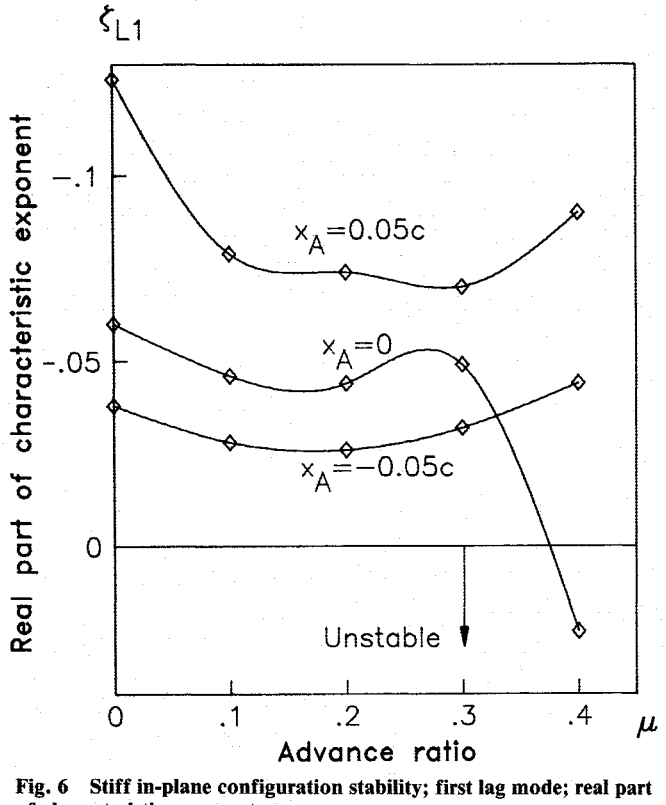

Fig. 6 Stiff in-plane configuration stability; first lag mode; real part of characteristic exponent vs μ.

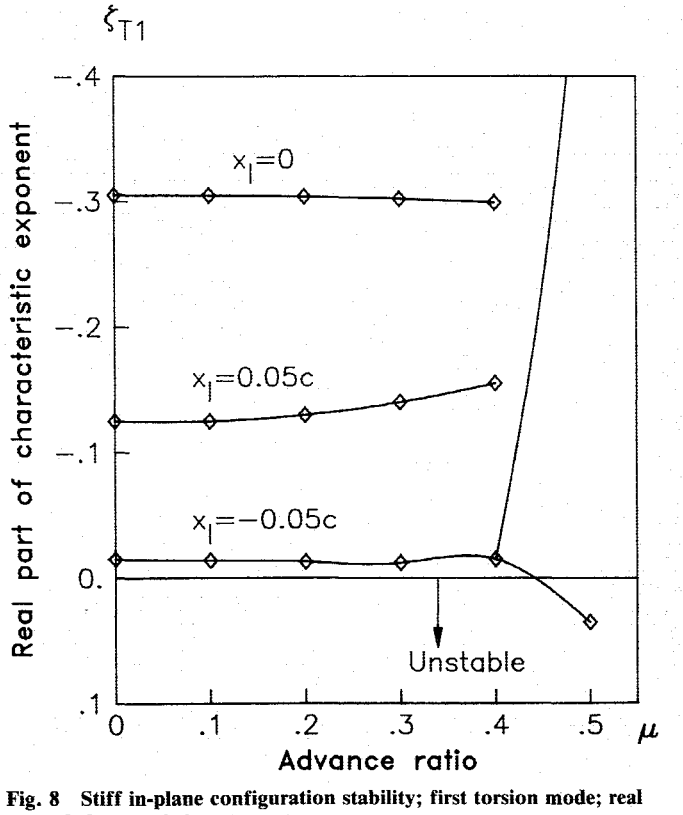

Fig. 8 Stiff in-plane configuration stability; first torsion mode; real part of characteristic exponent vs μ.

Previous research[1-4] showed that the critical degree of freedom in the coupled flap-lag-torsional dynamics of a hingeless blade is associated with the first lag mode. Thus, the aeroelastic stability of the blade is represented, usually, by plotting the real part of the characteristic exponent of this degree of freedom as a function of the advance ratio.

Figure 4 shows the real part ζ_{L1} of the characteristic exponent of the first lag mode as a function of the advance ratio μ. The blade is stable if $\zeta_{L1} < 0$. The figure shows that moving the center of mass ahead of the elastic axis ($x_I > 0$) has a stabilizing effect, and it eliminates the lag mode instability that can be observed for the range of advance ratios considered for $x_I = 0$. For the case $x_I < 0$, the stability of the system in the fundamental lag mode increases; however, the blade becomes unstable in torsion. For conciseness, the behavior of the torsional characteristic exponent is not shown

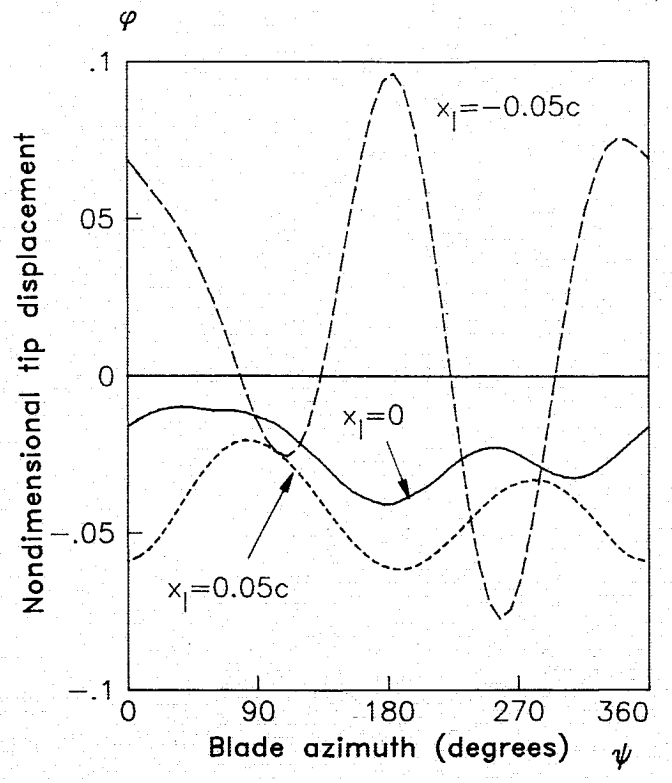

Fig. 9 Soft in-plane blade configuration; torsional response of the blade tip; advance ratio $\mu = 0.4$.

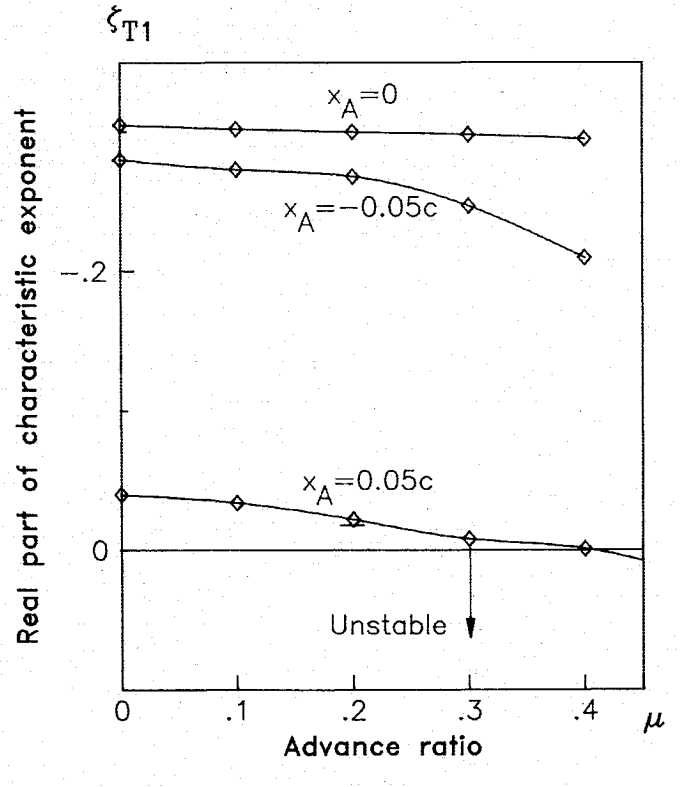

Fig. 10 Soft in-plane configuration stability; first torsion mode; real part of characteristic exponent vs μ.

here; however, it can be found in Ref. 27.

Figure 5 shows the torsional deformation of the blade tip as a function of the azimuth angle ψ. The detrimental effect of moving the center of mass behind the elastic axis is clearly indicated by the drastic increase in torsional response that occurs for $x_I < 0$.

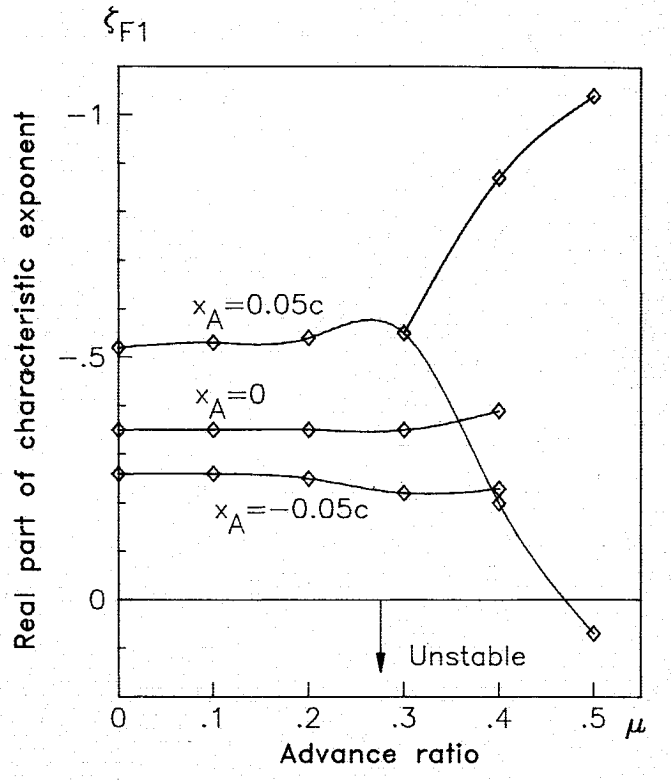

Fig. 11 Soft in-plane configuration stability; first flap mode; real part of characteristic exponent vs μ.

Figure 6 and 7 show some effects of moving the aerodynamic center (AC) of the cross section away from the elastic axis. Results are presented for three stiff in-plane blade configurations: one in which the elastic axis and the aerodynamic center coincide, a second with a positive AC-EA offset x_A equal to 5% of the blade chord, and the third with the same amount of offset, but negative. The AC-EA offset x_A is positive if the AC is ahead of the EA. Except for the offsets, these configurations are the same as those in Figs. 4 and 5.

Figure 7 shows the torsional deformation of the blade tip as a function of the blade azimuth angle ψ. Moving the aerodynamic center ahead of the elastic axis produces large torsional responses, in a manner which is quite similar to that obtained by moving the center of mass behind the elastic axis.

Figures 8 and 9 show results for three soft in-plane blade configurations: one with coincident CG and EA, a second with a positive CG-EA offset x_I equal to 5% of the blade chord, and the third with the same amount of offset, but negative.

Figure 8 shows the real part ζ_{T1} of the characteristic exponent of the first torsion mode, as a function of the advance ratio μ. A negative x_I reduces the stability of the blade and triggers an instability for $\mu > 0.4$. A mild phenomenon of frequency coalescence between the first torsion and the second flap modes is also responsible for the degradation in stability that occurs for a nonzero CG-EA offset. The coupled rotating frequencies are 3.14/rev and 3.46/rev for the first torsion and second flap mode, respectively, and the CG-EA offset introduces significant torsional components in the second flap mode. Results not shown here[27] indicade a considerable increase in the damping of the second lag mode. Figure 9 shows the torsional deformation of the blade tip as a function of the azimuth angle ψ. As in the stiff in-plane case, moving the CG behind the EA leads to a sharp increase of the torsional response of the blade.

Figures 10 through 12 illustrate some of the effects of moving the aerodynamic center away from the elastic axis. Results are presented for three soft in-plane blade configuration, one in which the elastic axis and the aerodynamic center

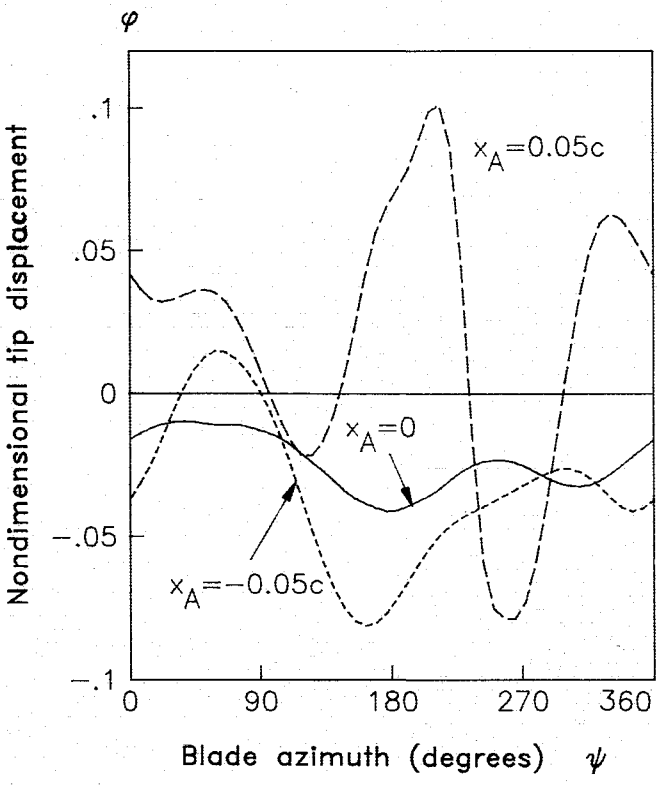

Fig. 12 Soft in-plane blade configuration; torsional response of the blade tip; advance ratio $\mu = 0.4$.

coincide, a second with a positive AC-EA offset x_A equal to 5% of the blade chord, and the third with the same amount of offset, but negative.

In Figs. 10 and 11, the real parts ζ_{T1} and ζ_{F1} of the characteristic exponent, for the first torsion and first flap mode, respectively, are shown as a function of the advance ratio μ. The usually well-damped first torsion mode is strongly destabilized by moving the AC behind the EA and becomes unstable for $\mu > 0.45$. Finally, Fig. 12 shows the torsional deformation of the blade tip as a function of the azimuth angle ψ. As in the stiff in-plane case, moving the AC ahead of the EA is very similar to that of moving the CG behind the EA. This is clearly evident from comparing these results with those of Fig. 9.

Conclusions

A new implementation of the aerodynamic loads has been presented in this paper. This formulation does not require that the expressions defining the aerodynamic loads be expanded symbolically. Furthermore, it also does not require that such expressions be explicit functions of the blade displacement quantities. The implementation effort is, therefore, considerably reduced, and more sophisticated aerodynamic models can easily be incorporated in the analysis. The implicit formulation, coupled with a finite-element discretization and a quasilinearization solution technique, provides a new, flexible tool for rotary wing aeroelastic analyses.

The computer program implementing the new formulation was validated successfully and used to study the aeroelastic stability and response of rotor blades with noncoincident elastic axes, centers of gravity, and aerodynamic centers. The results of this study show the following.

1) Moving the center of gravity ahead of the elastic axis increases the blade stability and removes the lag instability typical of stiff in-plane blades at high advance ratios.

2) Moving the center of gravity behind the elastic axis sharply increases the torsional response of the blade and can make both soft and stiff in-plane blades torsionally unstable.

3) The effect of moving the aerodynamic center behind the elastic axis is qualitatively the same as that of moving the center of gravity ahead of the elastic axis.

4) These results also have implications when attempting to correlate full-scale or aeroelastic model tests with theoretical results. Since the precise location of the elastic axis or shear center sometimes is difficult to obtain or measure, it is quite possible that aeroelastic stability boundaries or aeroelastic response information obtained in tests and calculated from theory can differ, if such offsets are not properly taken into account.

Acknowledgments

This research was funded by NASA Grant NAG 2-226, Ames Research Center, Moffett Field, California. The support of the grant monitor, Dr. H. Miura, is gratefully acknowledged.

References

[1]Friedmann, P. P., "Recent Trends in Rotary-Wing Aeroelasticity," *Vertica,* Vol. 11, No. 1, 1987, pp. 139–170.

[2]Friedmann, P. P., "Formulation and Solution of Rotary-Wing Aeroelastic Stability and Response Problems," *Vertica,* Vol. 7, No. 2, 1983, pp. 101–141.

[3]Johnson, W., "Recent Developments in the Dynamics of Advanced Rotor Systems," *Vertica,* Vol. 10, No. 1, Pt. 1, 1986, pp. 72–107, and Vol. 10, No. 2, Pt. 2, 1986, pp. 109–150.

[4]Ormiston, R. A., "Investigation of Hingeless Rotor Stability," *Vertica,* Vol. 7, No. 2, 1983, pp. 143–182.

[5]Friedmann, P. P. and Straub, F. K., "Application of the Finite Element Method to Rotary-Wing Aeroelasticity," *Journal of the American Helicopter Society,* Vol. 25, Jan. 1980, pp. 36–44.

[6]Straub, F. K. and Friedmann, P., "A Galerkin Type Finite Element Method for Rotary-Wing Aeroelasticity in Hover and Forward Flight," *Vertica,* Vol. 5, No. 1, 1981, pp. 75–98.

[7]Straub, F. K. and Friedmann, P., "Application of the Finite Element Method to Rotary-Wing Aeroelasticity," NASA CR-165854, Feb. 1982.

[8]Sivaneri, N. T. and Chopra, I., "Dynamic Stability of a Rotor Blade Using Finite Element Analysis," *AIAA Journal,* Vol. 20, May 1982, pp. 716–723.

[9]Chopra, I., "Aeroelastic Analysis of an Elastic Circulation Control Rotor Blade in Hover," *Vertica,* Vol. 8, No. 4, 1984, pp. 353–371.

[10]Sivaneri, N. T. and Chopra, I., "Finite Element Analysis for Bearingless Rotor Blade Aeroelasticity," *Journal of the American Helicopter Society,* Vol. 29, No. 2, April 1984, pp. 42–51.

[11]Panda, B. and Chopra, I., "Dynamic Stability of Hingeless and Bearingless Rotors in Forward Flight," *Computers and Mathematics with Applications,* Vol. 12A, Jan. 1986, pp. 111–130.

[12]Hong, C.-H. and Chopra, I., "Aeroelastic Stability Analysis of a Composite Rotor Blade," *Journal of the American Helicopter Society,* Vol. 30, No. 2, April 1985, pp. 57–67.

[13]Chopra, I., "Dynamic Stability of a Bearingless Circulation Control Rotor Blade in Hover," *Journal of the American Helicopter Society,* Vol. 30, No. 4, Oct. 1985, pp. 40–47.

[14]Bir, G. S. and Chopra, I., "Gust Response of Hingeless Rotors," *Journal of the American Helicopter Society,* Vol. 31, No. 2, April 1986, pp. 33–46.

[15]Hodges, D. H., Hopkins, A. S., Kunz, D. L., and Hinnant, H. E., "Introduction to GRASP—General Rotorcraft Aeromechanical Stability Program—A Modern Approach to Rotorcraft Modeling," *Journal of the American Helicopter Society,* Vol. 32, No. 2, April 1987, pp. 78–90.

[16]Hodges, D. H., Hopkins, A. S., and Kunz, D. L., "Analysis of Structures with Rotating, Flexible Substructures Applied to Rotorcraft Aeroelasticity in GRASP," AIAA Paper 87-0952, April 1987.

[17]Nagabhushanam, J., Gaonkar, G. H., and Reddy, T. S. R., "Automatic Generation of Equations for Rotor-Body Systems with Dynamic Inflow for A Priori Ordering Schemes," *Proceedings of the 7th European Rotorcraft Forum,* Garmish-Partenkirchen, FRG, 1981.

[18]Reddy T. S. R., "Flap-Lag Damping of an Elastic Rotor Blade with Torsion and Dynamic Inflow in Hover from Symbolically Generated Equations," AIAA Paper 84-0980, May 1984.

[19]Reddy T. S. R. and Warmbrodt, W., "The Influence of Dynamic

Inflow and Torsional Flexibility on Rotor Damping in Forward Flight from Symbolically Generated Equations," *Proceedings of the Second Decennial Specialists Meeting on Rotorcraft Dynamics,* NASA Ames Research Center, Moffett Field, CA, NASA CP-2400, Nov. 1985, pp. 221–239.

[20]Gibbons, M. P. and Done, G. T. S., "Automatic Generation of Helicopter Rotor Aeroelastic Equations of Motion," *Vertica,* Vol. 8, No. 3, 1984, pp. 229–241.

[21]Patel, M. H. and Done, G. T. S., "Experience With a New Approach to Rotor Aeroelasticity," *Vertica,* Vol. 9, No. 3, 1985, pp. 285–294.

[22]Friedmann, P. and Kottapalli, S. B. R., "Coupled Flap-Lag-Torsional Dynamics of Hingeless Rotor Blades in Forward Flight," *Journal of the American Helicopter Society,* Vol. 27, No. 4, Oct. 1982, pp. 28–36.

[23]Shampine, L. F. and Gordon, M. K., *Computer Solution of Ordinary Differential Equations—The Initial Value Problem,* W. H. Freeman and Co., San Francisco, CA, 1975.

[24]Shampine, L. F., Watts, H. A., and Davenport, S. M., "Solving Nonstiff Ordinary Differential Equations—The State of the Art," *SIAM Review,* Vol. 18, No. 3, July 1976, pp. 376–411.

[25]Press, W. H., Flannery, B. P., Teukolsky, S. A., and Vetterling, W. T., *Numerical Recipes—The Art of Scientific Computing,* Cambridge Univ. Press, Cambridge, England, 1986, pp. 596–572.

[26]Peters, D. A. and Hohenemser, K. H., "Application of the Floquet Transition Matrix to the Problem of Lifting Rotor Stability," *Journal of the American Helicopter Society,* Vol. 16, No. 2, April 1971, pp. 25–33.

[27]Celi, R., *Aeroelasticity and Structural Optimization of Helicopter Rotor Blades With Swept Tips,* Ph.D. Dissertation, Mechanical, Aerospace, and Nuclear Engineering, Univ. of California, Los Angeles, CA, Oct. 1987.